

Supplementary Figure 1: Analysis of transcriptional start sites (TSS) and features of active Group 3 tumor enhancers.

A-B. Heatmaps (A) and Examples (B) depicting categories of TSS observed in tumors: Active, Bivalent and Repressed. H3K4me3 ChIP-seq signals are shown in blue and H3K27me3 in red. Active sites have H3K4m3 alone, Repressed sites have H3K27me3 alone and Bivalent sites have both marks. The number of TSS are 13297, 3205, 774, 5523 for the Active, Repressed, Bivalent and None categories.

C. Active genes identified by their TSS chromatin state are more highly expressed in Group 3 tumors. Boxplots depict aggregate RNA-seq levels (FPKM) in five primary tumor samples in each category (Active/Bivalent/Repressed and None).

D. Number of H3K27ac peaks detected in each primary tumor. Left: Total peaks. Right: Putative enhancers based on annotation with a 2 kb window around Refseq promoters.

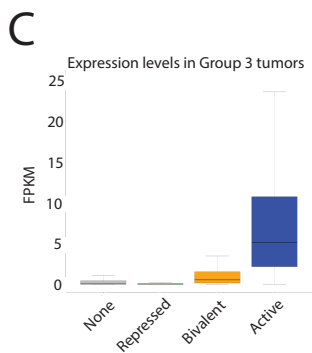
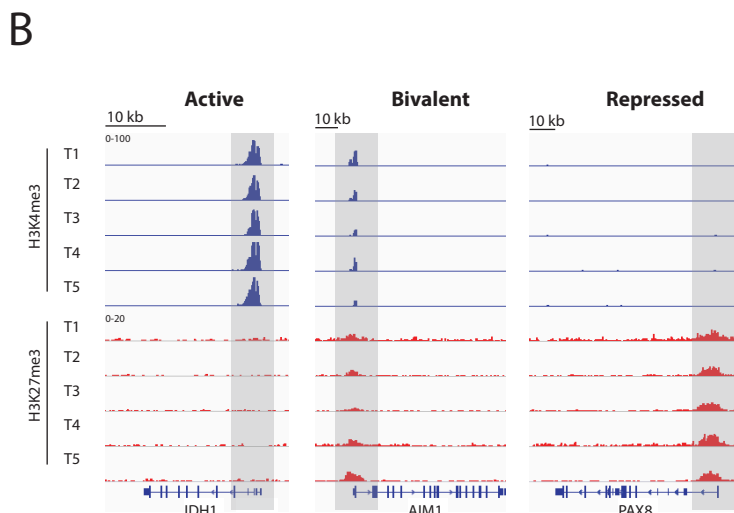
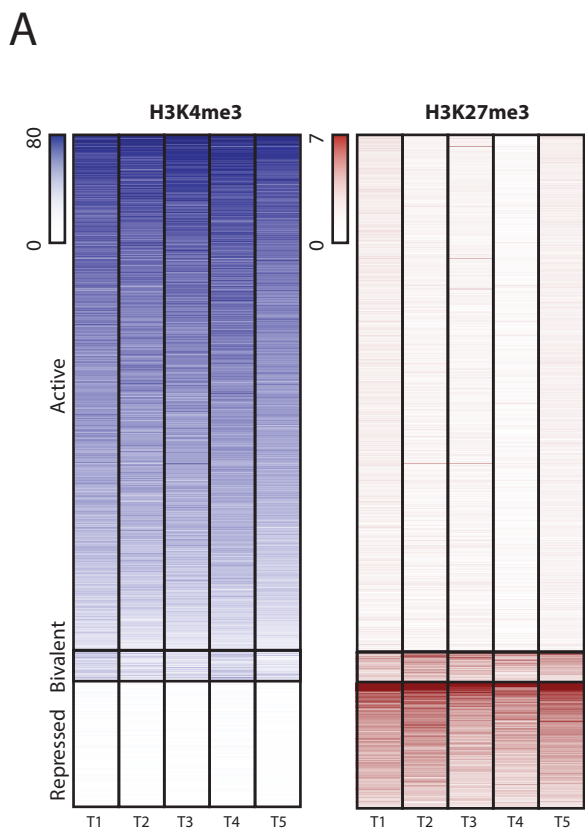
E. Bar chart shows the number of H3K27ac peaks shared by primary tumors.

F. Histogram plot shows the size distribution of 9621 Group 3 active enhancers present in 4 out of 5 tumor samples. The median and average size are indicated.

G. Pie chart shows annotations for 9621 Group 3 active enhancers present in 4 out of 5 samples using Homer.

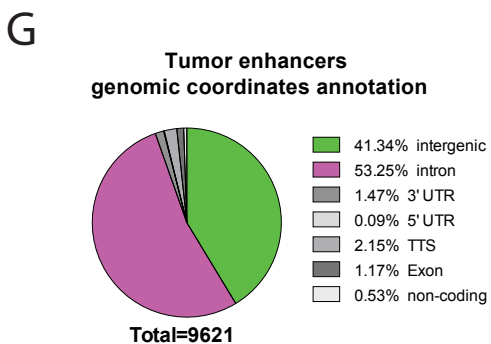
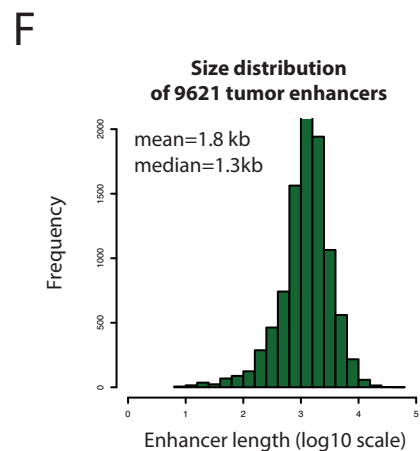
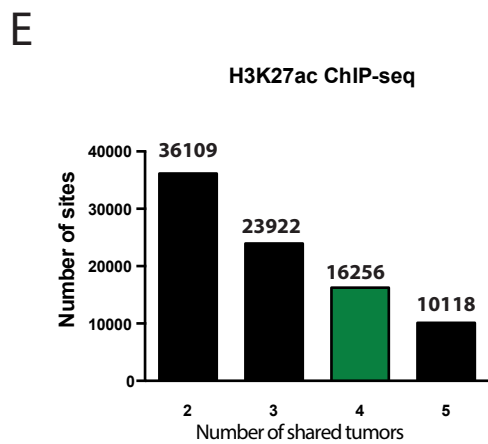
H. Number of H3K27ac peaks in each cell line. Left: Total peaks. Right: Putative enhancers based on annotation with a 2 kb window around Refseq promoters.

I. Bar chart shows the percentage of 9621 Group 3 active enhancers sites containing significant H3K27ac signal in each cell line.



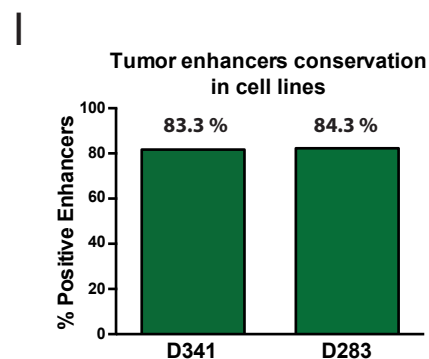
D

Tumor sample	#H3K27ac Peaks	#Putative Enhancers
T1	30333	20082
T2	25229	18094
T3	26872	18365
T4	34529	25539
T5	32423	23099



H

cell line	#H3K27ac Peaks	#Putative Enhancers
D341	34951	26561
D283	31333	24057



Supplementary Figure 2: Motif analysis of active Group 3 medulloblastoma enhancers highlights OTX2 as the most significant hit.

Putative enhancers identified in each primary tumor were used for motif discovery analyses separately (T1-T5). Putative enhancers in cell lines were also tested. OTX2 was the top enriched motif in each analysis.

	Motif 1	Motif 2	Motif 3
T1	<p>OTX2</p> <p>p=1e-408</p>	<p>NEUROD1</p> <p>p=1e-215</p>	<p>NF1</p> <p>p=1e-167</p>
T2	<p>OTX2</p> <p>p=1e-507</p>	<p>NEUROD1</p> <p>p=1e-492</p>	<p>NF1</p> <p>p=1e-224</p>
T3	<p>OTX2</p> <p>p=1e-832</p>	<p>NEUROD1</p> <p>p=1e-433</p>	<p>CRX</p> <p>p=1e-199</p>
T4	<p>OTX2</p> <p>p=1e-1307</p>	<p>NEUROD1</p> <p>p=1e-420</p>	<p>CRX</p> <p>p=1e-347</p>
T5	<p>OTX2</p> <p>p=1e-771</p>	<p>NF1</p> <p>p=1e-313</p>	<p>NEUROD1</p> <p>p=1e-225</p>
D341	<p>OTX2</p> <p>p=1e-1245</p>	<p>NF1</p> <p>p=1e-348</p>	<p>NEUROD1</p> <p>p=1e-345</p>
D283	<p>OTX2</p> <p>p=1e-1125</p>	<p>NF1</p> <p>p=1e-363</p>	<p>CRX</p> <p>p=1e-323</p>

Supplementary Figure 2 Boulay et al.

Supplementary Figure 3: ATAC-seq in D283 cells also highlights OTX2 as the most significant enriched motif.

A. Pie chart shows annotations for ATAC-seq peaks in D283 cells based on the Refseq promoter database (2 kb window) and H3K4me3 ChIP-seq data.

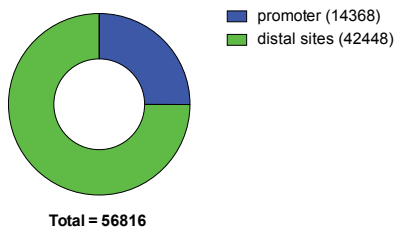
B. Pie chart shows detailed annotations for ATAC-seq peaks at distal sites.

C. OTX2 is the most significant enriched motif in a motif analysis of ATAC-seq distal sites.

D. Examples of ATAC-seq signals in D283 cells at shared active Group 3 enhancers. ATAC-seq signals are shown in black. Coordinates for the active enhancer set defined in tumors are shown in green.

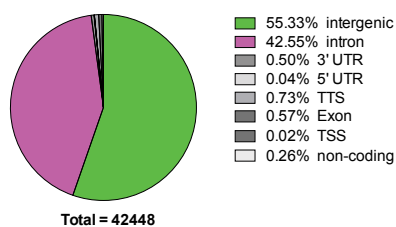
A

ATAC-seq Peaks in D283



B

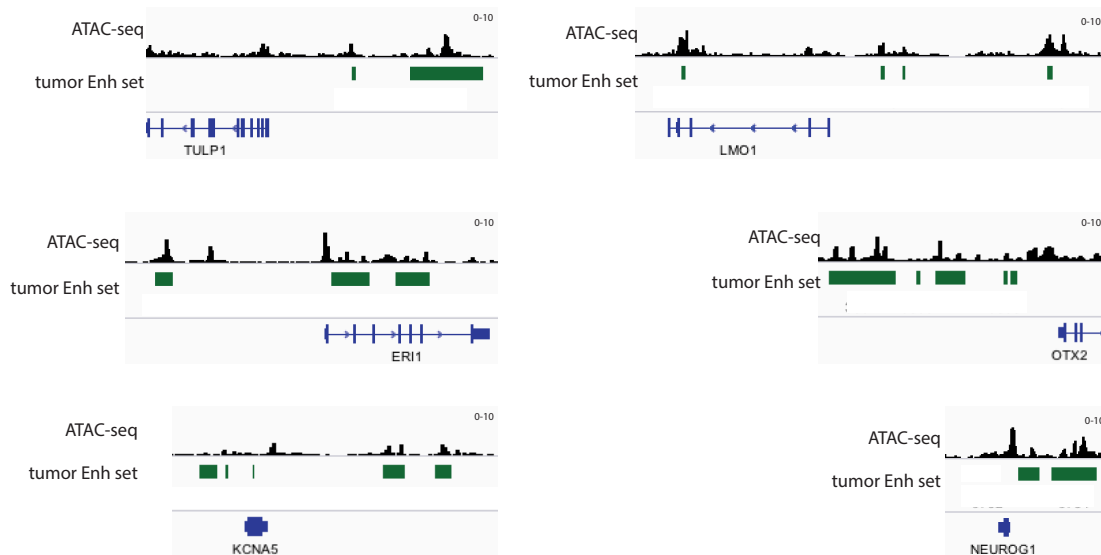
ATAC-seq distal sites annotation



C

	Motif 1	Motif 2	Motif 3
D283 ATAC-seq	OTX2  p=1e-4554	CRX  p=1e-3773	NF1  p=1e-1212

D



Supplementary Figure 4: Characterization of OTX2 binding sites and identification of a subset of active OTX2 bound enhancers specific to Group 3 tumors.

A. Bar chart shows overlap between four OTX2 ChIP-seq peak sets obtained using two antibodies in two cell lines (D283 and D341).

B. Pie chart shows annotations for OTX2 putative enhancer sites using Homer.

C. OTX2 bound promoters are mostly active. Heatmaps show OTX2 (purple), H3K4me3 (blue) and H3K27me3 (red) ChIP-seq signals in D341 and D283 cell lines and ATAC-seq (black) in D283. Each row shows a 10 kb region centered on OTX2 binding sites and ordered based on average H3K4me3 levels.

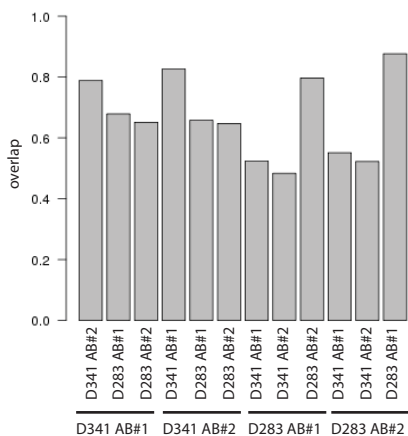
D. OTX2 bound distal sites show a wide range of H3K27ac levels. Heatmaps depict OTX2 (purple), H3K4me1 (blue) and H3K27ac (green) ChIP-seq signals in cell lines and ATAC-seq (black) in D283. Each row shows a 10 kb region centered on OTX2 binding sites and ordered based on the average H3K27ac levels in cell lines.

E. A large fraction of OTX2 bound Group 3 enhancers are also active in non-SHH medulloblastoma. Histograms show the average H3K27ac ChIP-seq levels in tumors at OTX2 bound Group 3 enhancers defined in Figure 1G (2kb window).

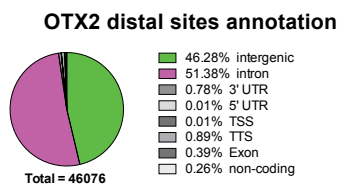
F. A subset of OTX2 bound tumor enhancers is Group 3 specific. A barplot shows the overlap among medulloblastoma subtypes for OTX2 bound Group 3 enhancers with high average H3K27ac ChIP-seq signals.

G. Genes nearest to Group 3 specific OTX2 bound enhancers tend to be more highly expressed in Group 3 medulloblastoma tumors. A heatmap shows z-scores of expression values for 705 closest genes in primary medulloblastoma samples.

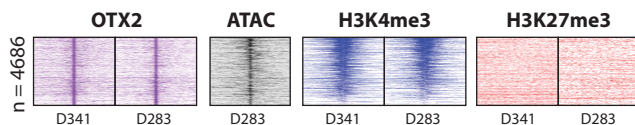
A



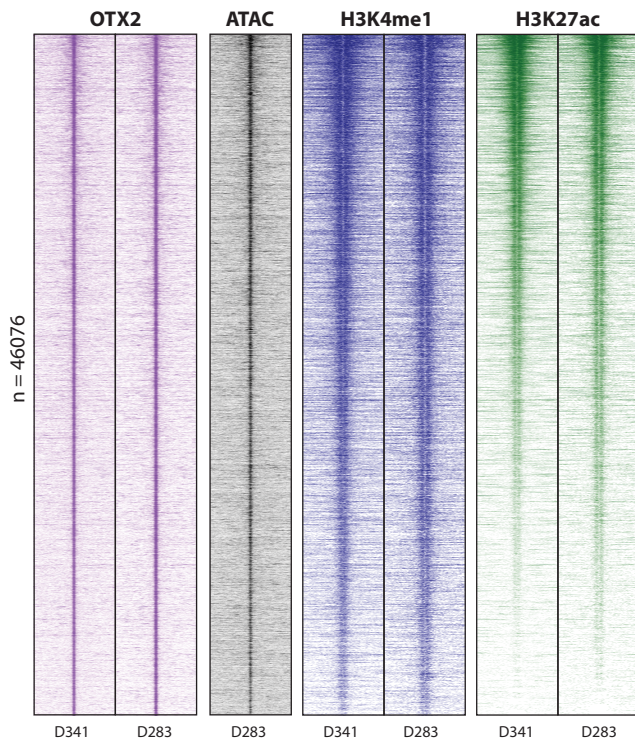
B



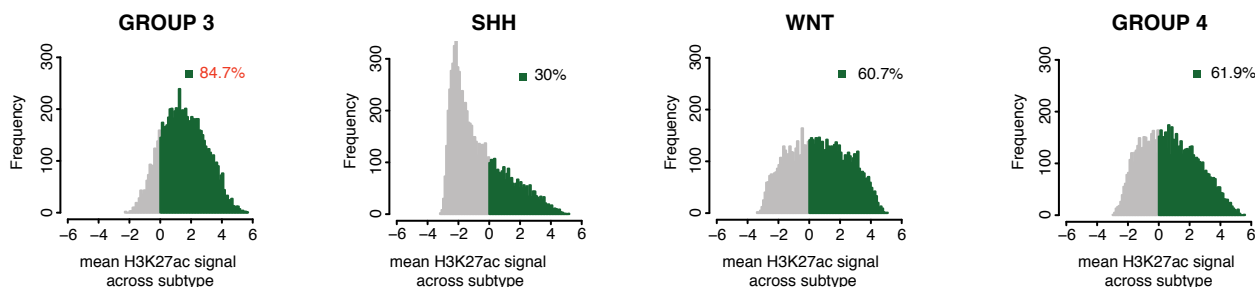
C



D

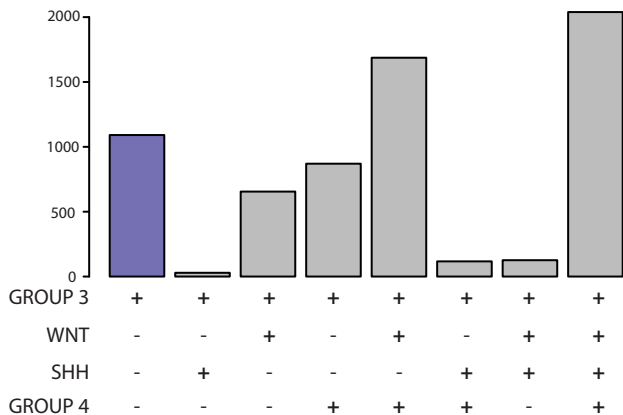


E

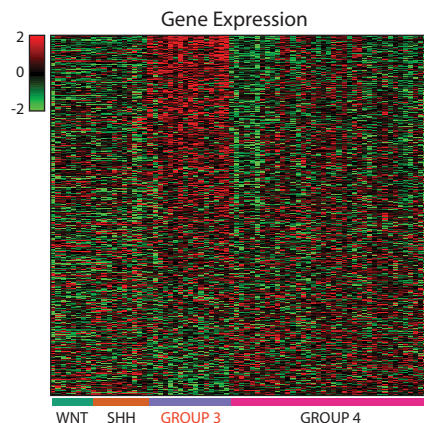


F

Overlap of OTX2 bound active Group 3 enhancers with active sites among medulloblastoma subtypes



G



Supplementary Figure 5: Further characterization of OTX2 binding sites.

A. Patterns of H3K27ac levels observed at distal OTX2 binding sites in cell lines are conserved in primary tumors. Boxplots show combined H3K27ac ChIP-seq levels in 5 primary Group 3 tumors at genomic coordinates of OTX2 sites with different levels of H3K27ac in cell lines. *** Indicates p value < 1e-20.

B. Boxplots show H3K27ac, H3K4me1, OTX2 ChIP-seq and ATAC-seq average signals on the two categories of OTX2 binding sites identified in Figure 2E. Active sites (yellow) and Inactive sites (green). H3K27ac and H3K4me1 (2kb windows), OTX2 and ATAC-seq (variable window corresponding to the OTX2 binding site). Large differences are seen only for H3K27ac. Scales show log₂ signal intensity. p values for each pair (Active sites in yellow and Inactive sites in green) < 1e-20.

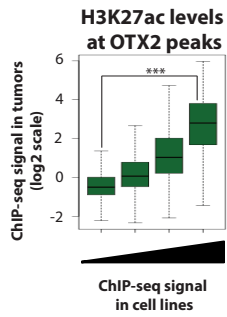
C. Boxplots showing H3K27ac and H3K4me1 ChIP-seq average signals in Group 3 tumors on the two categories of OTX2 binding sites identified in Figure 2A (2 kb windows). Active sites (yellow) and Inactive sites (green). Large differences are seen for H3K27ac. Scales show log₂ signal intensity. p values for each pair (Active sites in yellow and Inactive sites in green) < 1e-20.

D. Heatmaps depict H3K4me1 ChIP-seq (blue) in cell lines and Group 3 tumors. Each row shows a 10 kb region centered on OTX2 binding sites and ordered based on the average H3K27ac levels in D341 and tumors in Figure 2E: Active sites (top; n=7053) and Inactive sites (bottom; n=5751). On the right, the green and yellow rectangles mark the Active and Inactive OTX2 binding sites respectively.

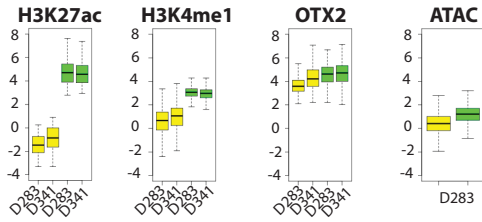
E. Motif analysis of active OTX2 distal sites highlights NEUROD1 as the most significant hit. Motif analysis comparing Active vs Inactive OTX2 binding sites.

F. OTX2 is associated with higher activity at NEUROD1 binding sites. A boxplot shows H3K27ac ChIP-seq levels at NEUROD1 peaks in presence or absence of OTX2. Categories were selected for low levels (n= 2020) or high levels (n= 2632) of OTX2 ChIP-seq signal at NEUROD1 distal sites in D341 cells. *** Indicates p value < 1e-20.

A

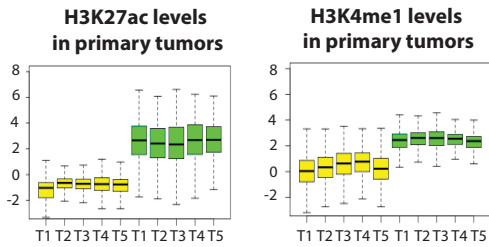


B

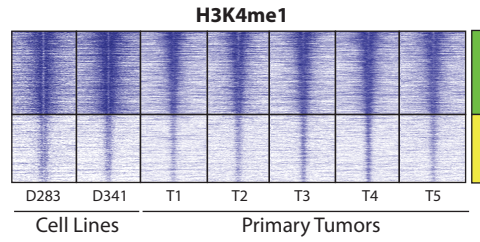


Active sites Inactive sites

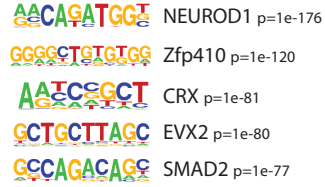
C



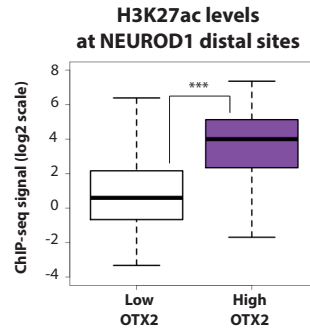
D



E



F



Supplementary Figure 6: OTX2 and NEUROD1 are required for medulloblastoma survival and distal site activity.

A. *OTX2* knockdown affects medulloblastoma cell growth. Cell viability assays 7 days post-infection with lentiviral shRNAs targeting *OTX2* in D341 and D283. ** Indicates p value < 0.01.

B. *OTX2* knock-out affects medulloblastoma cell growth. Cell viability assays 7 days post-infection with lentiviral guide RNA and Cas9 targeting the *OTX2* locus in D341. ** Indicates p value < 0.01.

C. Immunoblotting for *OTX2* in D283 knockdown experiments shows a decrease in *OTX2* protein levels.

D. Depletion of *OTX2* has a strong effect on chromatin states of Active *OTX2* sites compared to Inactive sites. Histograms show changes in H3K27ac at sites with decreased *OTX2* after infection of D283 medulloblastoma cells with shRNA lentiviruses. Left: H3K27ac decreases in Active sites after *OTX2* depletion (n=2991). Right: Inactive sites are mostly unaffected by *OTX2* depletion (n=3173). The red line indicates no variation; blue bars correspond to more than two-fold decrease and red bars to more than two-fold increase.

E. *OTX2* immunoblotting in D341 knock-out experiments.

F. *OTX2* loss by CRISPR-Cas9 targeting also leads to decreased H3K27ac signals at bound enhancers. Heatmap depicts significant H3K27ac ChIP-seq changes at 13398 sites with decreased *OTX2* after infection with lentiviral guide RNA and Cas9.

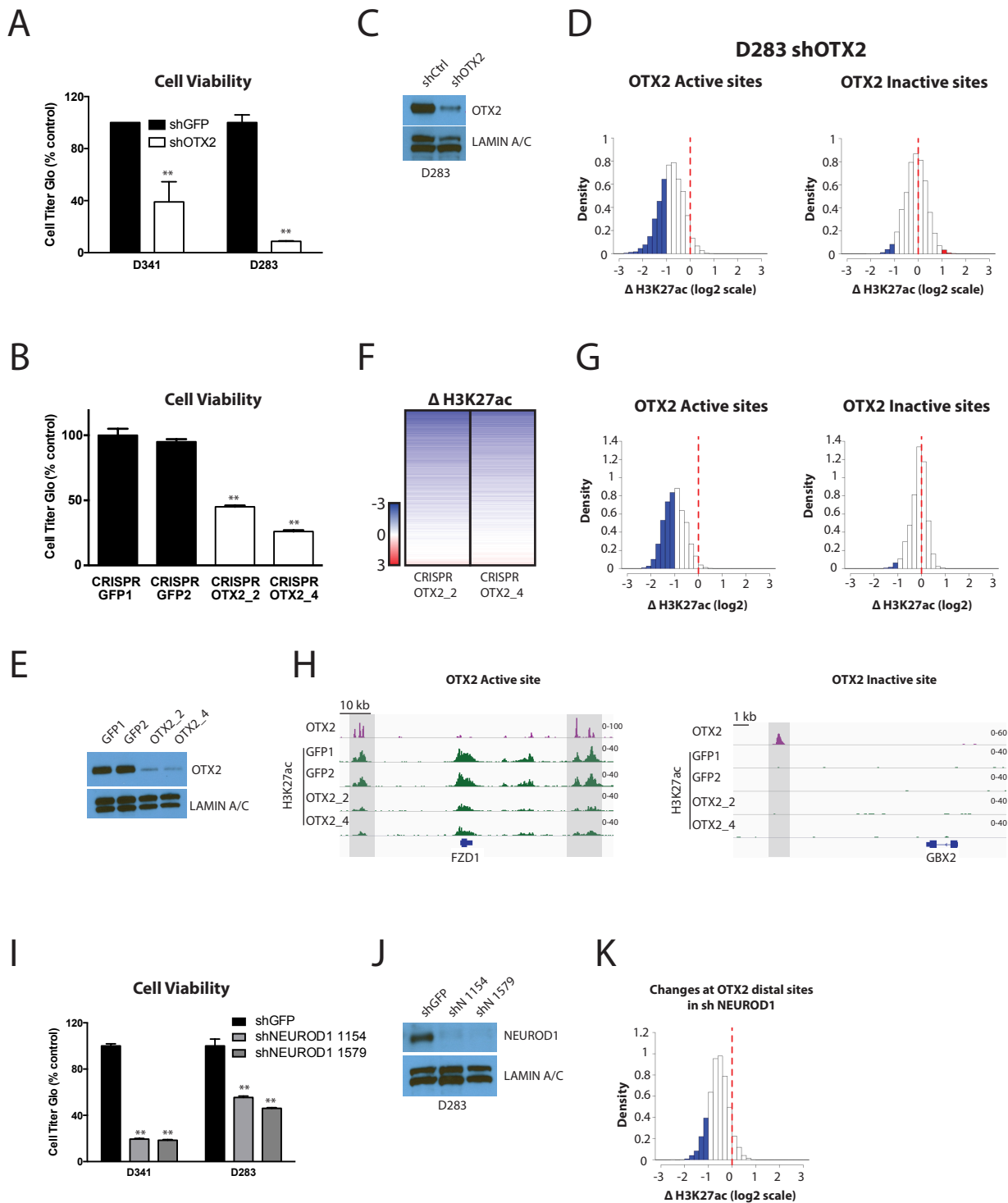
G. Active *OTX2* sites are sensitive to CRISPR-Cas9 mediated *OTX2* loss. Histogram plots depict H3K27ac ChIP-seq changes at sites with decreased *OTX2* after infection with lentiviral guide RNA and Cas9 targeting. Left: Major H3K27ac decreases are seen on Active sites in absence of *OTX2* (n= 1667). Right: Inactive sites are mostly not affected (n= 1599). The red line indicates no variation; blue bars correspond to more than two-fold decrease and red bars to more than two-fold increase.

H. ChIP-seq tracks showing examples of H3K27ac changes at *OTX2* distal sites following *OTX2* knock-out in D341 cells. *OTX2* in purple and H3K27ac in green. Regions of interest are shown in light gray.

I. *NEUROD1* knockdown affects medulloblastoma cell growth. Cell viability assays 7 days post-infection with lentiviral shRNA targeting *NEUROD1* in D341 and D283 cells. ** Indicates p value < 0.01.

J. Immunoblotting for *NEUROD1* in D283 knockdown experiments.

K. Depletion of *NEUROD1* affects chromatin states at *OTX2* bound enhancers. Histogram plot shows H3K27ac ChIP-seq changes at *OTX2* distal sites with decreased *NEUROD1* after infection of D283 medulloblastoma cells with lentiviral shRNA (3283 sites are shown). The red line indicates no variation; blue bars correspond to more than two-fold decrease and red bars to more than two-fold increase.



Supplementary Figure 7: OTX2 can operate as a pioneer factor.

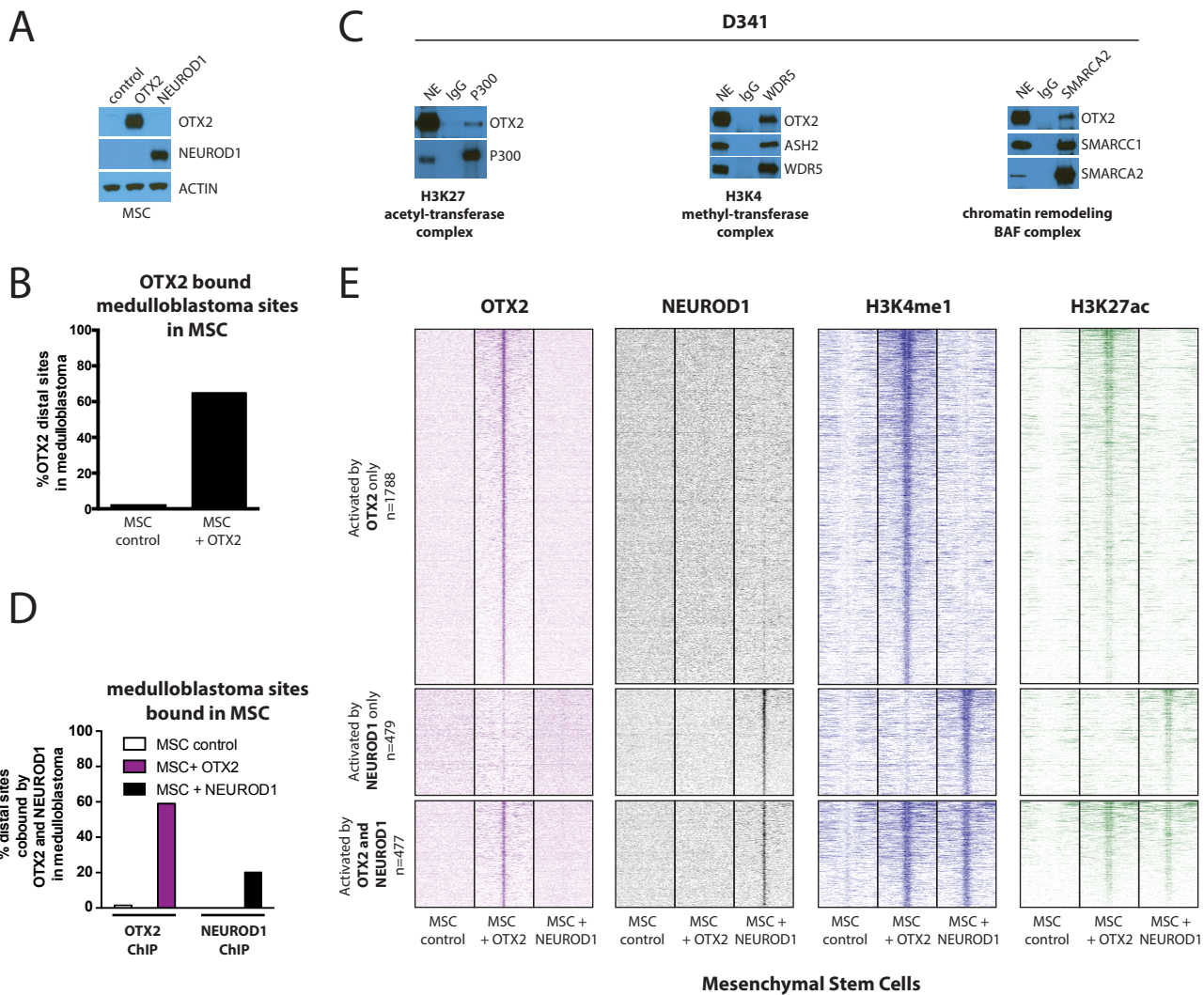
A. Expression of ectopic OTX2 and NEUROD1 proteins detected using immunoblotting in MSCs after lentiviral infection.

B. Expression of ectopic OTX2 with a lentiviral vector in mesenchymal stem cells (MSCs) results in binding to a majority of OTX2 sites found in Medulloblastoma. Barplot shows the percentage of OTX2 distal sites identified in medulloblastoma that are bound by OTX2 in mesenchymal stem cells after lentiviral infection. n=65% of 46117 distal sites.

C. OTX2 interacts with chromatin modifying complexes. Reverse co-immunoprecipitation experiments in D341 nuclear extracts for p300, WDR5 and SMARCA2.

D. Barplot shows the percentage of distal sites cobound by OTX2 and NEUROD1 identified in Group 3 medulloblastoma cell lines that are bound by OTX2 or NEUROD1 in mesenchymal stem cells after lentiviral infection. Of 9847 distal sites 59% are bound by OTX2 and 20% are bound by NEUROD1.

E. OTX2 can activate more medulloblastoma enhancers *de novo* in MSCs than NEUROD1. Heatmaps depict OTX2 (purple), NEUROD1 (black), H3K4me1 (blue) and H3K27ac (green) ChIP-seq signals on *de novo* enhancers 72 hours after lentiviral-induced expression in MSCs. Each row shows a 10 kb region centered on OTX2/NEUROD1 co-bound distal sites identified in Group 3 medulloblastoma.



Supplementary Figure 8: *NEK2* expression is sensitive to OTX2 levels in medulloblastoma.

A. GSEA analysis of OTX2 responsive genes identified in Figure 4B. OTX2 target genes are enriched in cell cycle pathways that include the mitotic kinase *NEK2*.

B. A subset of OTX2 responsive genes is significantly more highly expressed in tumors. Heatmap showing z-scores of expression values for matching genes in normal cerebellum and Group 3 medulloblastoma.

C. Boxplot showing *NEK2* expression levels in normal cerebellum and Group 3 medulloblastoma samples.

D. ChIP-seq tracks show OTX2 (purple) and H3K27ac (green) on the *NEK2* locus in D341 cells 5 days after infection with lentiviral shRNA targeting *OTX2*. RNA-seq tracks are shown in blue. Regions of interest are shown in light gray.

E. *NEK2* expression is sensitive to OTX2 levels. RT-qPCR measuring *NEK2* mRNA levels in D341 5 days post-infection with lentiviral guide RNA and Cas9 targeting *OTX2* locus. ** Indicates p value < 0.01.

F. *NEK2* knock-down efficiency. (Left) *NEK2* expression levels were measured by RT-qPCR in D341 and D283 cells five days post-infection with three specific shRNAs targeting *NEK2*. ** Indicates p value < 0.01. (Right) *NEK2* Immunoblotting in the same conditions.

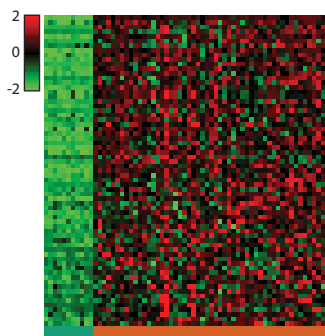
G. Histogram showing cell type specific sensitivity to shRNA mediated knockdown of *NEK2* (Project Achilles). 216 cell lines are ordered by shRNA score, which is defined as the normalized log₂ fold change in shRNA abundance relative to the initial DNA reference pool. Sensitive cell lines have a negative shRNA score.

A

Hallmark Gene Sets (GSEA)

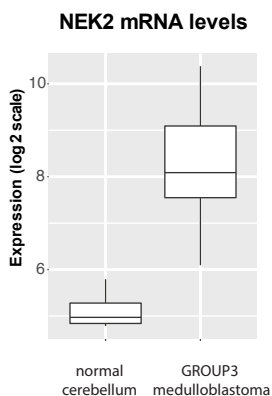
Gene set	p-value	FDR q-value	# genes	
cell cycle related targets of E2F transcription factors	2.31 e-8	2.88 e-7	14	KIF4A, RFC1, HMGB2, WEE1, CDC25A, CDKN3, POLA2, CCNE1, RPA3, DCK, DNMT1, MRE11A, DIAPH3, CDCA3
mitotic spindle assembly	2.31 e-8	2.88 e-7	14	KIF4A, RFC1, NOTCH2, NEDD9, NEK2 , TPX2, MYO1E, SPTBN1, VCL, ECT2, CDC42EP4, FGD6, PXN, KNTC1
G2/M checkpoint	7.67 e-6	3.49 e-5	11	KIF4A, CDC25A, CDKN3, POLA2, NOTCH2, NEK2 , TPX2, SMAD3, CCNF, DMD, KPNB1

B

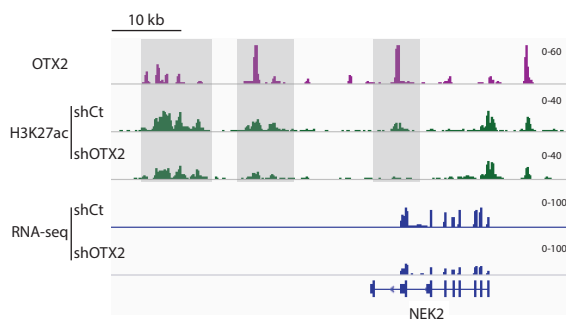


normal cerebellum GROUP3 medulloblastoma

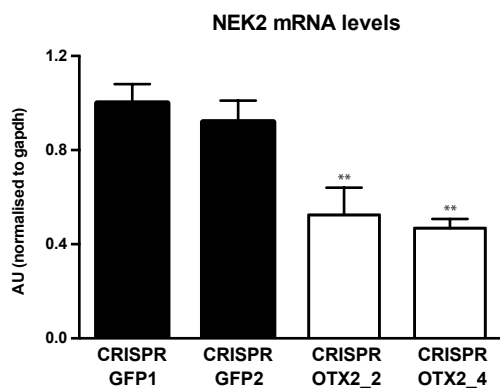
C



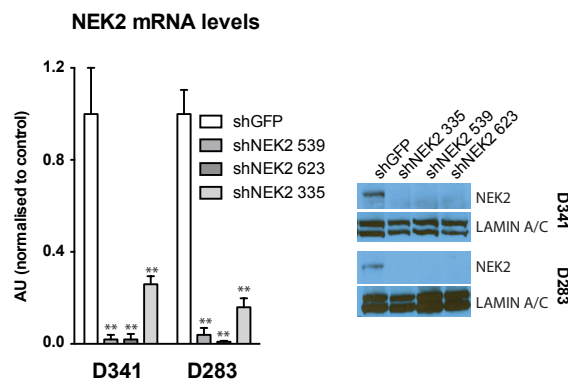
D



E



F



G

